To be published in Optics Letters:

Title:	Extended depth of focus for Transmission X-ray Microscope
Authors:	Yijin Liu, Junyue Wang, Youli Hong, Zhili Wang, Kai Zhang, Phillip Williams, Peiping Zhu, Joy Andrews, Piero Pianetta, and Ziyu Wu
Accepted:	30 July 2012
Posted:	1 August 2012
Doc. ID:	170837

Extended depth of focus for Transmission X-ray Microscope

Yijin Liu,[1,5,6] Junyue Wang,[2,5] Youli Hong,[3,5] Zhili Wang,[4] Kai Zhang,[3] Phillip A. Williams,[1] Peiping Zhu,[3] Joy C. Andrews,[1] Piero Pianetta[1] and Ziyu Wu[4,3,7]

[1] *Stanford Synchrotron Radiation Lightsource, SLAC National Accelerator Laboratory, Menlo Park, CA 94025, USA*
[2] *HPSynC, Carnegie Institution of Washington, 9700 S Cass Avenue, Argonne, Illinois 60439, USA*
[3] *Beijing Synchrotron Radiation Facility, Institute of High Energy Physics, Beijing 100049, China*
[4] *National Synchrotron Radiation Laboratory, University of Science and Technology of China, Hefei 230027, China*
[5] *These authors contributed equally to this Letter*
[6] *liuyijin@slac.stanford.edu*
[7] *wuzy@ustc.edu.cn*

Compiled July 31, 2012

A Fast Discrete Curvelet Transform based focus-stacking algorithm for extending the depth of focus of a transmission X-ray microscope (TXM) is presented. By analyzing an image stack of a sample taken in a Z-scan, a fully in-focus image can be generated by the proposed scheme. With the extended depth of focus, it is possible to obtain 3D structural information over a large volume at nanometer resolution. The focus-stacking method has been demonstrated using a dataset taken with a laboratory X-ray source based TXM system. The possibility and limitations of generalizing this method to a synchrotron based TXM are also discussed. We expect the proposed method to be of important impact in 3D X-ray Microscopy. © 2012 Optical Society of America

OCIS codes: 110.7440, 180.7460.

The Fresnel zone plate based Transmission X-ray Microscope (TXM) has been well recognized as one of the most powerful tools for non-invasive investigation of the inner structure of thick samples, with spatial resolution down to 15-30 nm [1, 2]. Thanks to the development of the nanofabrication technique [3], x-ray zone plates can be designed and fabricated to work at different energy levels, covering a wide energy range from the "water window" [4] to around 25 keV [5]. As a result, Transmission X-ray Microscopes for both hard and soft X-rays have been reported at different facilities around the world [1, 2, 4–14]. Many studies about the methodology and applications based on TXM system, including quantitative phase retrieval methods in TXM and biological study of cells using TXM, have also been presented [15–19]. While higher spatial resolutions are attained with the use of Fresnel zone plates characterized by larger diameter and smaller outermost zone width, the Depth-Of-Focus (DOF) of the objective zone plate decreases. The typical DOF of a water window soft x-ray TXM is below 10 μm [13, 14] for 60 nm resolution and decreases to about 1 μm for 20 nm resolution; while the corresponding value for a hard x-ray TXM operating at 8 keV is about 40 μm [1]. With continued improvement in spatial resolution, the DOF is further reduced. A small DOF can be considered as an advantage in performing optical sectioning [2], however, it is considered as an important limitation for the reconstruction volume in 3D tomographic imaging since the DOF can be substantially smaller than the field-of-view (FOV) of the microscope.When mosaic TXM images of large samples are collected using raster sample scanning [1,8] this DOF limitation becomes even more significant.

In this Letter, we present a Fast Discrete Curvelet Transform [20, 21] based algorithm for extending the DOF (also known as focus-stacking) [22] by analyzing the image stack taken in a sample scan along the optical axis. The feasibility of the method is confirmed with experimental data collected using a laboratory source based hard X-ray TXM system (nanoXCT by Xradia, Inc.). The possibility for application of the method using a synchrotron radiation based TXM system is also discussed.

The images were collected using a full-field transmission hard X-ray microscopy system installed at beamline 4W1A at the Beijing Synchrotron Radiation Facility (BSRF). The schematic experimental setup is shown in Fig.1. Either synchrotron radiation or a rotating anode X-ray source can be used to illuminate an object in the TXM. In this experiment, we used an 8 keV X-ray beam generated from a Rigaku 007 HF rotating Cu anode (Cu-K emission line) with 70 μm spot size. A capillary condenser with a beam-stop is used to produce a hollow cone illumination beam and focused to a spot of 50 μm at the object plane. A pinhole, installed between the exit window of the condenser chamber and the sample stage, was used to shape the illumination beam to reduce unwanted X-rays. A pair of stacked Fresnel zone plates of 75 μm diameter, 40 nm outermost-zone-width and measured combined efficiency of 12.2% was installed as the objective lens to achieve a magnification factor of about 45 in addition to the magnification achieved by the internal objective lens in the optical camera. The camera system consisted of a thin, high-efficiency scintillator crystal optically coupled to a Helium-cooled 1024 by 1024 pixel CCD detector (Photonics CCD) with 13 μm pixel size, corresponding to about 15.1 nm pixel size in the sample plane. The field of view was 15 μm by 15 μm, with a spatial resolution better than 50 nm as determined by the analysis of an Au Siemens test pattern.

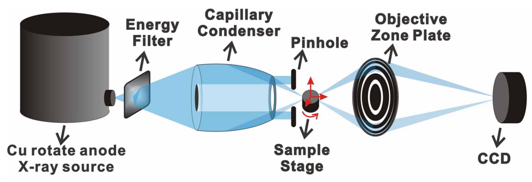

Fig. 1. Schematic experimental setup of the TXM installed at beamline 4W1A at the Beijing Synchrotron Radiation Facility.

The depth of focus of the TXM system for diffraction limited imaging is related to the numerical aperture of the objective zone plate, quantitatively given by the following equation:

$$\mathrm{DOF} = \pm\frac{\lambda}{2\mathrm{NA}^2} = \pm\frac{2\Delta r_n^2}{\lambda} \tag{1}$$

in which NA is the numerical aperture of the zone plate; λ is the wavelength of the incident X-ray; Δr_n is the outermost zone width of the objective zone plate. With our geometrical parameters we estimate a depth of focus of ± 20.8 μm for diffraction limited imaging.

The specimen was constructed from two layers of 75 μm-thick polyimide membranes, each labeled with micro-sized Au particles on both sides, thus giving three separate layers of Au microparticles spanning approximately 150 μm along the propagation axis.It was significantly thicker than the DOF of the TXM system, resulting in both image blurring and a phase contrast effect due to the off-focal propagation for certain parts of the specimen. Transmission X-ray images were collected at a series of Z positions by scanning the sample along the optical axis with 15 μm sample Z motor step size of over a range of about 650 μm, ensuring that all features were in focus in at least one of the images of the entire stack. Four representative images from our sample Z scan are presented in Fig. 2. As shown in this figure, the sample Z scan was begun at a position where the sample was completely off-focus, stepping through the in-focus positions of the front and back surfaces of the membrane, ending in a position where the sample was again off-focus.

In this work we proposed a Fast Discrete Wavelet Transform based on the focus-stacking algorithm to compose a fully-in-focus image from the image stack collected with a sample Z scan along the optical train. The three main steps of the focus-stacking algorithm are illustrated in Fig. 3(a), with a magnified view of the composite fully-in-focus image shown in Fig. 3(b). We emphasize here that the two Au particles marked with arrows in Fig 3(b) are on the same side of the membrane as the bottom-right particle cluster [indicated in Figs. 2(b) and 2(c)].

A detailed description of the algorithm can be illustrated in 4 steps as following: **(i)** A phase correlation

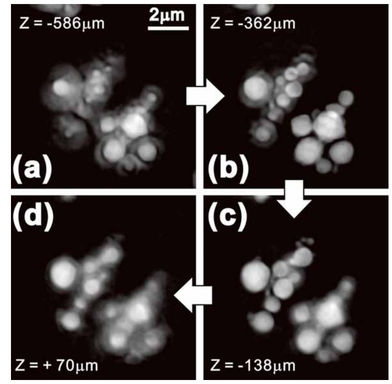

Fig. 2. Sample Z scan for a test sample significantly thicker than the DOF of the TXM system. Panel (a) shows a transmission X-ray image at a position where all the Au particles are off-focus; panel (b) and (c) are images taken at positions where the front and back surface is in focus, respectively; panel (d) corresponds position where all the particles are out of focus again. The intensity in the images represents the absorption coefficient of the sample.

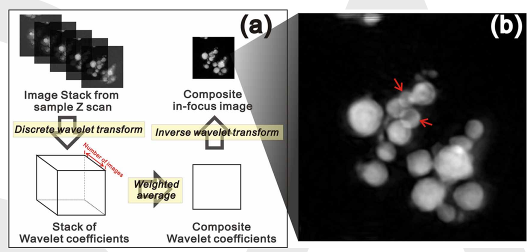

Fig. 3. Data processing algorithm to extend DOF by analyzing the image stack collected in a sample Z scan along the optical train is illustrated in panel (a). Panel (b) is a magnified view of the composite fully-in-focus image.

algorithm [23] based on auto image alignment is used to correct errors due to possible misalignment of the sample Z motor with respect to the optical axis. **(ii)** A 2D Fast Discrete Wavelet Transform [20–22] is performed for each image in the stack:

$$FDWT\left(img\left(x,y,z\right)\right) = \left\{c_j\left(n,m,z\right)\right\}_j \tag{2}$$

in which $FDWT$ is the 2D Fast Discrete Wavelet Transform function; img is the 3D matrix of the image stack; z is the index of the images and c_j is the wavelet coefficient at scale j. **(iii)** A weighted average of the wavelet coefficients' stack is used to generate the composite wavelet coefficients set. The weighting factor is related to the normalized amplitude value of the wavelet coefficients, and is given by:

$$W_j\left(n,m,z\right) = \frac{\left|c_j\left(n,m,z\right)\right|^k}{\sum\limits_z \left|c_j\left(n,m,z\right)\right|^k} \tag{3}$$

in which W is the weighting factor; k is a positive integral depending on the image contrast and the signal to noise ratio. **(iv)** An inverse wavelet transform leads to the fully-in-focus image:

$$img_{infoc} = \left| \mathrm{IFDWT}\left(\sum_{z} \{c_j(n,m,z)\}_j \cdot W_j(n,m,z) \right) \right| \tag{4}$$

where $IFDWT$ is the inverse 2D Fast Discrete Wavelet Transform function and img_{infoc} is the output image which is fully-in-focus.

The result presented in this letter was collected with a Cu rotating anode. The exposure time was 180 seconds with 2 by 2 pixel binning. Using the BSRF as X-ray source, the required exposure time would be reduced by a factor of about 20. It can be even shorter using a third generation synchrotron X-ray source (such as the SSRL). However, when using a synchrotron the off-focal Fresnel fringes will be enhanced due to the spatial coherence, resulting in sharper contour and complicating the focus-stacking procedure. One way to overcome the problem is to install a spinning X-ray diffuser in the imaging system to blur the effects of spatial coherence.

In summary, we presented a focus-stacking algorithm to extend the depth-of-focus of a TXM. Based on the Fast Discrete Wavelet Transform method, the algorithm generates a fully-in-focus image by analyzing the image stack taken in a sample Z scan along the optical axis. The proposed method has been demonstrated using a data set collected using TXM system coupled to a laboratory X-ray source. Possibility and limitations of the method using a synchrotron X-ray source based TXM were discussed. This proposed function has also been included in a freely available software package [24].

Acknowledgement

The authors gratefully acknowledge Wenbing Yun, Michael Feser, Florian Meirer, Johanna Nelson, and Jun-Sik Lee for valuable discussions. This work was partly supported by the National Basic Research Program of China (2012CB825800, 2009CB930804), the Knowledge Innovation Program of the Chinese Academy of Sciences ($KJCX2-YW-N42$), and the Key Important Project of the National Natural Science Foundation of China (10734070), and. The TXM project at the Stanford Synchrotron Radiation Light Source was support by NIH/NIBIB grant number 5R01EB004321. The SSRL is supported by the U.S. Department of Energy, Office of Science.

References

1. J. C. Andrews, E. Almeida, M. C. H. van der Meulen, J. S. Alwood, C. Lee, Y. Liu, J. Chen, F. Meirer, M. Feser, J. Gelb, J. Rudati, A. Tkachuk, and W. Yun, Microsc. Microanal. **16,** 327–336, (2010).
2. W. Chao, B. D. Harteneck, J. A. Liddle, E. H. Anderson, and D. T. Attwood, Nature **435,** 1210-1213 (2005).
3. W. Yun, B. Lai, Z. Cai, J. Maser, D. Legnini, E. Gluskin, Z. Chen, A. A. Krasnoperova, Y. Vladimirsky, F. Cerrina, E. Di Fabrizio, and M. Gentili, Rev. Sci. Instrum. **70,** 2238 (1999).
4. M. A. Le Gros, G. McDermott, and C. A. Larabell, Curr. Opin. Struct. Biol. **15,** 593-600 (2005).
5. M. Awaji, Y. Suzuki, A. Takeuchi, H. Takano, N. Kamijo, S. Tamura, and M. Yasumoto, J. Synchrotron Radiat. **9,** 125-127 (2002).
6. G. C. Yin, M. T. Tang, Y. F. Song, F. R. Chen, K. S. Liang, F. W. Duewer, W. Yun, C. H. Ko, and H. P. D. Shieh, Appl. Phys. Lett. **88,** 241115 (2006).
7. W. Li, N. Wang, J. Chen, G. Liu, Z. Pan, Y. Guan, Y. Yang, W. Wu, J. Tian, S. Wei, Z. Wu, Y. Tian, and L. Guo, Appl. Phys. Lett. **95,** 053108 (2009).
8. G. B. Kim, Y. J. Yoon, T. J. Shin, H. S. Youn, Y. S. Gho, and S. J. Lee, Microsc. Res. Tech. **71,** 639-643 (2008).
9. Y. S. Chu, J. M. Yi, F. De Carlo, Q. Shen, W. K. Lee, H. J. Wu, C. L. Wang, J. Y. Wang, C. J. Liu, C. H. Wang, S. R. Wu, C. C. Chien, Y. Hwu, A. Tkachuk, W. Yun, M. Feser, K. S. Liang, C. S. Yang, J. H. Je, and G. Margaritondo, Appl. Phys. Lett. **92,** 103119 (2008).
10. A. Tkachuk, F. Duewer, H. Cui, M. Feser, S. Wang, W. Yun, Z. Kristallogr **222,** 650-655 (2007).
11. U. Neuhausler, G. Schneider, W. Ludwig, M. A. Meyer, E. Zschech, and D. Hambach, J. Phys. D: Appl. Phys. **36,** A79-A82 (2003).
12. S. Rehbein, S. Heim, P. Guttmann, S. Werner, and G. Schneider, Phys. Rev. Lett. **103,** 110801 (2009).
13. W. Meyer-Ilse, D. Hamamoto, A. Nair, S. A. Lelivre, G. Denbeaux, L. Johnson, A. L. Pearson, D. Yager, M. A. Legros, and C. A. Larabell, J. Microsc. **201,** 395-403 (2001).
14. G. Schneider, P. Guttmann, S. Heim, S. Rehbein, F. Mueller, K. Nagashima, J. B. Heymann, W. G. Mller, and J. G. McNally, Nature Methods **7,** 985-987 (2010).
15. G. C. Yin, F. R. Chen, Y. Hwu, H. P. D. Shieh, and K. S. Liang, Appl. Phys. Lett. **90,** 181118 (2007).
16. Y. Liu, J. C. Andrews, J. Wang, F. Meirer, P. Zhu, Z. Wu, and P. Pianetta, Opt. Express **19,** 540-545(2011).
17. J. Chen, Y. Yang, X. Zhang, J. C. Andrews, P. Pianetta, Y. Guan, G. Liu, Y. Xiong, Z. Wu, and Y. Tian, Anal Bioanal. Chem. **397,** 2117-2121 (2010).
18. J. C. Andrews, S. Brennan, Y. Liu, P. Pianetta, E. A. C. Almeida, M. C. H. van der Meulen, Z. Wu, Z. Mester, L. Ouerdane, J. Gelb, M. Feser, J. Rudati, A. Tkachuk, and W. Yun, J. Phys. Condens. Matter. **186,** 12081 (2009).
19. D. Y. Parkinson, G. McDermott, L. D. Etkin, M. A. Le Gros, C. A. Larabell, J. Struct. Biol. **162,** 380-386 (2008).
20. E. J. Cands and D. L. Donoho, Comm. Pure Appl. Math. **57,** 219-266 (2004).
21. E. Cands, L. Demanet, D. Donoho, and L. Ying, Multiscale Model. Simul. **5,** 861-899 (2006).
22. B. Forster, D. van de Ville, J. Berent, D. Sage, and M. Unser, Microsc. Res. Tech. **65,** 33-42 (2004).
23. B. S. Reddy and B. N. Chatterji, IEEE Trans. Image Process. **5,** 1266-1271 (1996).
24. Y. Liu, F. Meirer, P. A. Williams, J. Wang, J. C. Andrews, and P. Pianetta, J. Synchrotron Rad. **19,** 281-287 (2012).

Informational Fourth Page

References

1. J. C. Andrews, E. Almeida, M. C. H. van der Meulen, J. S. Alwood, C. Lee, Y. Liu, J. Chen, F. Meirer, M. Feser, J. Gelb, J. Rudati, A. Tkachuk, and W. Yun, "Nanoscale X-ray Microscopic Imaging of Mammalian Mineralized Tissue," Microsc. Microanal. **16,** 327–336, (2010).
2. W. Chao, B. D. Harteneck, J. A. Liddle, E. H. Anderson, and D. T. Attwood, "Soft X-ray microscopy at a spatial resolution better than 15 nm," Nature **435,** 1210-1213 (2005).
3. W. Yun, B. Lai, Z. Cai, J. Maser, D. Legnini, E. Gluskin, Z. Chen, A. A. Krasnoperova, Y. Vladimirsky, F. Cerrina, E. Di Fabrizio, and M. Gentili, "Nanometer focusing of hard x rays by phase zone plates," Rev. Sci. Instrum. **70,** 2238 (1999).
4. M. A. Le Gros, G. McDermott, and C. A. Larabell, "X-ray tomography of whole cells," Curr. Opin. Struct. Biol. **15,** 593-600 (2005).
5. M. Awaji, Y. Suzuki, A. Takeuchi, H. Takano, N. Kamijo, S. Tamura, and M. Yasumoto, "Zernike-type X-ray imaging microscopy at 25 keV with Fresnel zone plate optics," J. Synchrotron Radiat. **9,** 125-127 (2002).
6. G. C. Yin, M. T. Tang, Y. F. Song, F. R. Chen, K. S. Liang, F. W. Duewer, W. Yun, C. H. Ko, and H. P. D. Shieh, "Energy-tunable transmission x-ray microscope for differential contrast imaging with near 60 nm resolution tomography," Appl. Phys. Lett. **88,** 241115 (2006).
7. W. Li, N. Wang, J. Chen, G. Liu, Z. Pan, Y. Guan, Y. Yang, W. Wu, J. Tian, S. Wei, Z. Wu, Y. Tian, and L. Guo, "Quantitative study of interior nanostructure in hollow zinc oxide particles on the basis of nondestructive x-ray nanotomography," Appl. Phys. Lett. **95,** 053108 (2009).
8. G. B. Kim, Y. J. Yoon, T. J. Shin, H. S. Youn, Y. S. Gho, and S. J. Lee, "X-Ray Imaging of Various Biological Samples Using a Phase-Contrast Hard X-Ray Microscope," Microsc. Res. Tech. **71,** 639-643 (2008).
9. Y. S. Chu, J. M. Yi, F. De Carlo, Q. Shen, W. K. Lee, H. J. Wu, C. L. Wang, J. Y. Wang, C. J. Liu, C. H. Wang, S. R. Wu, C. C. Chien, Y. Hwu, A. Tkachuk, W. Yun, M. Feser, K. S. Liang, C. S. Yang, J. H. Je, and G. Margaritondo, "Hard-x-ray microscopy with Fresnel zone plates reaches 40 nm Rayleigh resolution," Appl. Phys. Lett. **92,** 103119 (2008).
10. A. Tkachuk, F. Duewer, H. Cui, M. Feser, S. Wang, W. Yun, "X-ray computed tomography in Zernike phase contrast mode at 8 keV with 50-nm resolution using Cu rotating anode X-ray source," Z. Kristallogr **222,** 650-655 (2007).
11. U. Neuhausler, G. Schneider, W. Ludwig, M. A. Meyer, E. Zschech, and D. Hambach, "X-ray microscopy in Zernike phase contrast mode at 4 keV photon energy with 60 nm resolution," J. Phys. D: Appl. Phys. **36,** A79-A82 (2003).
12. S. Rehbein, S. Heim, P. Guttmann, S. Werner, and G. Schneider, "Ultrahigh-Resolution Soft-X-Ray Microscopy with Zone Plates in High Orders of Diffraction," Phys. Rev. Lett. **103,** 110801 (2009).
13. W. Meyer-Ilse, D. Hamamoto, A. Nair, S. A. Lelivre, G. Denbeaux, L. Johnson, A. L. Pearson, D. Yager, M. A. Legros, and C. A. Larabell, "High resolution protein localization using soft X-ray microscopy," J. Microsc. **201,** 395-403 (2001).
14. G. Schneider, P. Guttmann, S. Heim, S. Rehbein, F. Mueller, K. Nagashima, J. B. Heymann, W. G. Mller, and J. G. McNally, "Three-dimensional cellular ultrastructure resolved by X-ray microscopy," Nature Methods **7,** 985-987 (2010).
15. G. C. Yin, F. R. Chen, Y. Hwu, H. P. D. Shieh, and K. S. Liang, "Quantitative phase retrieval in transmission hard x-ray microscope," Appl. Phys. Lett. **90,** 181118 (2007).
16. Y. Liu, J. C. Andrews, J. Wang, F. Meirer, P. Zhu, Z. Wu, and P. Pianetta, "Phase Retrieval using polychromatic illumination for Transmission X-ray Microscopy," Opt. Express **19,** 540-545(2011).
17. J. Chen, Y. Yang, X. Zhang, J. C. Andrews, P. Pianetta, Y. Guan, G. Liu, Y. Xiong, Z. Wu, and Y. Tian, "3D nanoscale imaging of the yeast, Schizosaccharomyces pombe, by full-field transmission X-ray microscopy at 5.4 keV," Anal Bioanal. Chem. **397,** 2117-2121 (2010).
18. J. C. Andrews, S. Brennan, Y. Liu, P. Pianetta, E. A. C. Almeida, M. C. H. van der Meulen, Z. Wu, Z. Mester, L. Ouerdane, J. Gelb, M. Feser, J. Rudati, A. Tkachuk, and W. Yun, "Full-field transmission x-ray microscopy for bio-imaging," J. Phys. Condens. Matter. **186,** 12081 (2009).
19. D. Y. Parkinson, G. McDermott, L. D. Etkin, M. A. Le Gros, C. A. Larabell, "Quantitative 3-D imaging of eukaryotic cells using soft X-ray tomography," J. Struct. Biol. **162,** 380-386 (2008).
20. E. J. Cands and D. L. Donoho, "New tight frames of curvelets and optimal representations of objects with piecewise C2 singularities," Comm. Pure Appl. Math. **57,** 219-266 (2004).
21. E. Cands, L. Demanet, D. Donoho, and L. Ying, "Fast Discrete Curvelet Transforms," Multiscale Model. Simul. **5,** 861-899 (2006).
22. B. Forster, D. van de Ville, J. Berent, D. Sage, and M. Unser, "Complex Wavelets for Extended Depth-of-Field: A New Method for the Fusion of Multichannel Microscopy Images," Microsc. Res. Tech. **65,** 33-42 (2004).
23. B. S. Reddy and B. N. Chatterji, "An FFT-based Technique for Translation, Rotation, and Scale-Invariant Image Registration," IEEE Trans. Image Process. **5,** 1266-1271 (1996).
24. Y. Liu, F. Meirer, P. A. Williams, J. Wang, J. C. Andrews, and P. Pianetta, J. Synchrotron Rad. **19,** 281-287 (2012).